Metabolic reprogramming augments potency of human pSTAT3–inhibited iTregs to suppress alloreactivity

Kelly Walton,[1] Mario R. Fernandez,[2] Elizabeth M. Sagatys,[3] Jordan Reff,[4] Jongphil Kim,[5] Marie Catherine Lee,[6] John V. Kiluk,[6] Jane Yuet Ching Hui,[7] David McKenna Jr.,[8] Meghan Hupp,[8] Colleen Forster,[9] Michael A. Linden,[8] Nicholas J. Lawrence,[10] Harshani R. Lawrence,[10] Joseph Pidala,[11] Steven Z. Pavletic,[12] Bruce R. Blazar,[13] Said M. Sebti,[14] John L. Cleveland,[2] Claudio Anasetti,[11] and Brian C. Betts[1]

[1]Division of Hematology, Oncology, and Transplantation, Department of Medicine, Masonic Cancer Center, University of Minnesota, Minneapolis, Minnesota, USA. [2]Department of Tumor Biology, [3]Department of Hematopathology and Laboratory Medicine, [4]Department of Immunology, [5]Department of Biostatistics and Bioinformatics, and [6]Department of Breast Oncology, Moffitt Cancer Center, Tampa, Florida, USA. [7]Department of Surgery, [8]Department of Laboratory Medicine and Pathology, and [9]Bionet Histology Research Laboratory, University of Minnesota, Minneapolis, Minnesota, USA. [10]Department of Drug Discovery and [11]Department of Blood and Marrow Transplantation and Cellular Immunotherapy, Moffitt Cancer Center, Tampa, Florida, USA. [12]Center for Cancer Research, National Cancer Institute, Bethesda, Maryland, USA. [13]Division of Blood and Marrow Transplantation, Department of Pediatrics, Masonic Cancer Center, University of Minnesota, Minneapolis, Minnesota, USA. [14]Department of Pharmacology and Toxicology, Virginia Commonwealth University, Richmond, Virginia USA.

Immunosuppressive donor Tregs can prevent graft-versus-host disease (GVHD) or solid-organ allograft rejection. We previously demonstrated that inhibiting STAT3 phosphorylation (pSTAT3) augments *FOXP3* expression, stabilizing induced Tregs (iTregs). Here we report that human pSTAT3–inhibited iTregs prevent human skin graft rejection and xenogeneic GVHD yet spare donor antileukemia immunity. pSTAT3-inhibited iTregs express increased levels of skin-homing cutaneous lymphocyte-associated antigen, immunosuppressive GARP and PD-1, and IL-9 that supports tolerizing mast cells. Further, pSTAT3-inhibited iTregs significantly reduced alloreactive conventional T cells, Th1, and Th17 cells implicated in GVHD and tissue rejection and impaired infiltration by pathogenic Th2 cells. Mechanistically, pSTAT3 inhibition of iTregs provoked a shift in metabolism from oxidative phosphorylation (OxPhos) to glycolysis and reduced electron transport chain activity. Strikingly, cotreatment with coenzyme Q10 restored OxPhos in pSTAT3-inhibited iTregs and augmented their suppressive potency. These findings support the rationale for clinically testing the safety and efficacy of metabolically tuned, human pSTAT3–inhibited iTregs to control alloreactive T cells.

Introduction

Human Tregs can suppress alloreactive T cells responsible for graft-versus-host disease (GVHD) and solid-organ allograft rejection (1–5). However, broadly suppressive calcineurin inhibitors (CNI) remain standard of care for preventing GVHD and allograft rejection, yet protection offered by CNIs is incomplete (6–8). Moreover, CNIs impair donor immunity and disrupt Treg function and survival, thus opposing durable immune tolerance (9, 10). Further, CNIs also increase the risk for opportunistic infections and secondary malignancies among transplant recipients (11).

In contrast, adoptive transfer of human Tregs has been shown safe, and emerging data have shown efficacy in preventing GVHD after allogeneic hematopoietic cell transplantation (alloHCT) (5, 12). Modification of standard GVHD prophylaxis regimens, such as incorporating mTOR inhibitors and/or low-dose IL-2, improves Treg reconstitution after alloHCT (9, 10, 13–16) and supports Treg persistence after adoptive transfer (12). Accordingly, contemporary phase I/II clinical trials are underway investigating the benefit of human Tregs in the prevention of GVHD and solid-organ transplant rejection (2, 15, 17, 18).

Clinical scale production of human Tregs is complex, requires local cell therapy expertise, and current good manufacturing practices–compliant (cGMP-compliant) protocols for Treg purification and expansion. The use of peripheral or "natural" Tregs versus induced Tregs is a key translational consideration. Peripheral Tregs are rare in circulation but offer reliable suppressive potency and phenotypic stability compared with induced Tregs (iTregs) (12, 19). However, circulating peripheral Tregs are scarce and raise the risk of production failure when using typical starting material for product manufacturing, like apheresis mononuclear cells. Conversely, iTregs are generated from a large and readily available pool of conventional T cells (Tconv), yet these have a theoretical risk of reverting to inflammatory Tconv (20). On the other hand, the large numbers of Tconv that can seed iTreg production mitigates hurdles regarding production. Thus, strategies to improve the phenotypic stability and potency of human iTregs are clearly warranted.

We have previously shown that STAT3 phosphorylation (pSTAT3) inhibition enhances the generation and phenotypic stability of human iTregs by provoking the demethylation of the Treg-specific demethylated region (TSDR) present in *FOXP3*, leading to increases in FOXP3 expression (21). As such, targeting pSTAT3 reduces the risk for Tconv reversion by the generated iTregs (21). Here we provide preclinical proof-of-concept evidence that adoptive transfer of human pSTAT3–inhibited iTregs have superior potency compared with control iTregs in suppressing alloreactive donor T cells, and in improving skin graft survival by limiting pathogenic T cell tissue invasion. Importantly, pSTAT3-inhibited iTregs reduce xenogeneic GVHD and preserve donor antileukemia immunity, a fundamental benefit of alloHCT.

Our human skin graft/NSG mouse xenotransplantation model is well suited to study human iTregs as the cells readily engraft in the immunodeficient mouse and skin is a clinically relevant organ in GVHD (22, 23). Skin is also a critical driver of alloreactivity and a well-established tissue to test experimental tolerance induction (24–26). Further, the model lends itself to the study of allospecific Tregs, as the Tregs are expanded with DCs from the skin donor.

Although targeting pSTAT3 significantly improves human iTreg potency, we demonstrate that pSTAT3 inhibition provokes a metabolic shift in iTregs from oxidative phosphorylation (OxPhos) toward glycolysis. We show cotreatment with coenzyme Q10 (CoQ10) restores OxPhos in pSTAT3-inhibited iTregs and further enhances their suppressive potency against alloreactive T cells. These findings support testing the safety and efficacy of metabolically tuned, human pSTAT3–inhibited iTregs in transplantation tolerance.

Results

Human pSTAT3–inhibited iTregs demonstrate superior suppressive potency. Human iTregs were generated as described previously, using Treg-depleted CD4$^+$ T cells stimulated by allogeneic DCs for 5 days (T/DC ratio 30:1) (21). The pSTAT3 inhibitor (27) S3i-201 (50 μM) or DMSO (<0.01%) was added once on day 0. The concentration of S3i-201 was previously optimized to potently suppress pSTAT3 while permitting pSTAT5 activity beneficial for Treg differentiation (21). Human recombinant IL-2 (10 IU/ml) was supplemented every other day. On day +5 of culture, the T cells were harvested and iTregs were purified by CD25$^+$ magnetic bead isolation. The final purity of the iTreg (CD4$^+$, CD127$^-$, CD25$^+$, Foxp3$^+$) (28, 29) product was >90% (Figure 1A). iTreg function was tested in standard suppression assays against DC-allostimulated T cells (22, 23, 30). Neither S3I-201 nor DMSO was added to the 5-day suppression assay cultures. The pSTAT3-inhibited iTregs demonstrated significant suppressive potency against DC-allostimulated T cells compared with DMSO-treated iTregs (Figure 1B). This enhanced iTreg suppression was achieved when either DC or bead stimulators were used during iTreg generation (Figure 1C), supporting the notion that the STAT3 inhibitor acts primarily on iTregs and not DCs. Silencing of human STAT3 during iTreg differentiation using a validated siRNA confirmed that inhibiting STAT3 augments their suppressive activity against alloreactive T cells in vitro (Figure 1D).

Mechanistically, the superior suppressive activity of pSTAT3-inhibited iTregs was associated with an increased frequency of GARP$^+$ and PD-1$^+$ iTregs (Figure 1, E–H). In contrast, the expression of other immunosuppressive molecules on iTregs, such as CD39, LAG3, and CTLA4 (Figure 1, I–K), was not affected by pSTAT3 inhibition. Upregulation of PD-1 and GARP in pSTAT3-inhibited iTregs was functionally relevant because neutralization of PD-1 or LAP/TGF-β1, the ligand for GARP (31, 32), with monoclonal antibodies significantly impaired the suppressive function of the pSTAT3-inhibited iTregs (Figure 1L). Conversely, inhibiting the CD39 ectonucleotidase with ARL67156 (30) had no effect on pSTAT3-inhibited iTreg potency (Figure 1L).
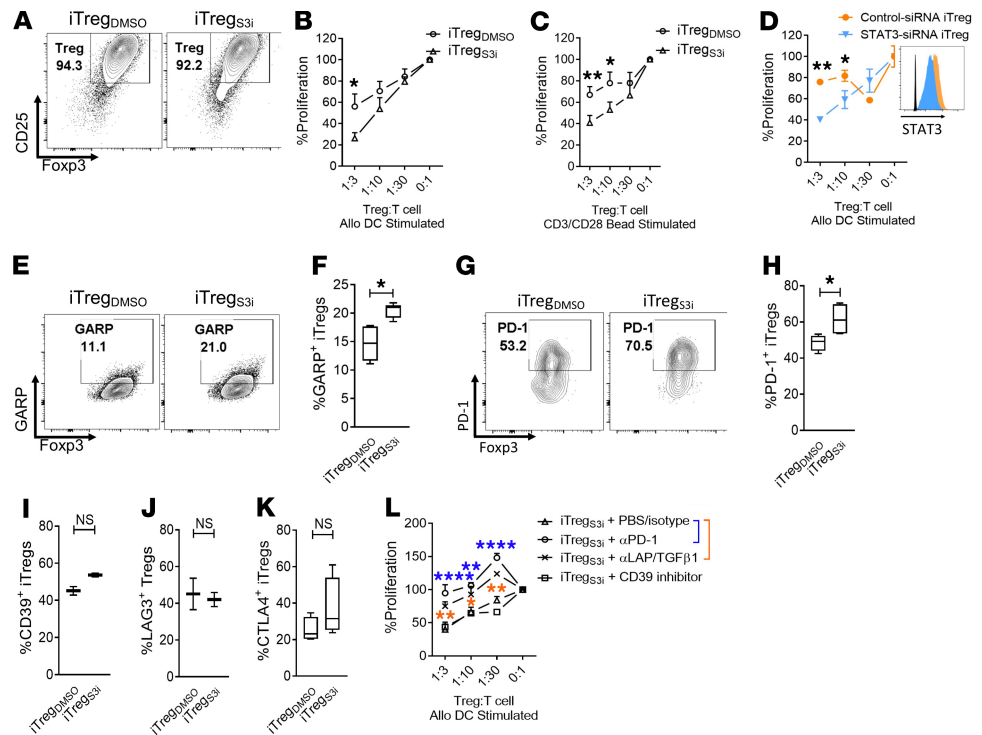
Figure 1. Human pSTAT3–inhibited iTregs demonstrate superior suppressive potency. (**A**) Contour plots show the purity of the generated CD4+ iTregs after CD25 selection using magnetic bead isolation. The suppressive potency of purified iTregs generated over 5 days with (**B**) allogeneic DC stimulators or (**C**) CD3/CD28 beads while exposed to S3i-201 (50 μM) or DMSO was tested at different ratios of iTreg to T cell responders in alloMLRs. No S3i-201 or DMSO was added to the suppression assay. Data are shown as mean ± SEM. *n* = 4 independent experiments. (**D**) The suppressive potency of iTregs generated with STAT3 or nontargeted siRNA (mean ± SEM) is shown. Histograms shows STAT3 expression in the nontargeted siRNA–treated iTregs (orange, gMFI 2870) and STAT3 siRNA–treated iTregs (blue, gMFI 1705). One of 2 independent experiments is shown. Contour plots and box-and-whisker plots (max, min, median) show the frequency of (**E** and **F**) GARP+, (**G** and **H**) PD-1+, and (**I–K**) CD39+, LAG3+, or CTLA4+ iTregs (CD4+, CD127−, CD25+, Foxp3+) after expansion with S3I-201 or DMSO from up to 5 independent experiments. (**L**) Graph shows the suppressive potency (mean ± SEM) of pSTAT3-inhibited iTregs treated with anti–human PD-1, LAP/TGF-β mAb, CD39 inhibitor ARL67156, or control (PBS plus isotype) from 1 of 2 independent experiments. ANOVA (**A**, **C**, **D**, and **L**) or paired *t* test (**F** and **H–K**). *$P < 0.05$, **$P = 0.001–0.01$, ****$P < 0.0001$. iTregs, induced Tregs; pSTAT3, STAT3 phosphorylation.

Human pSTAT3–inhibited iTregs significantly reduce skin graft rejection. Skin is an important and clinically relevant GVHD-target organ (33, 34). To test the activity of pSTAT3-inhibited iTregs in vivo, we used our established human skin graft/NSG mouse xenogeneic model (22, 23). NSG mice received a 1-cm² split thickness human skin graft. The mice rested for 30 days to permit skin graft healing and engraftment. During this time, human monocyte–derived DCs were generated from blood of the skin graft donor. These DCs were used to expand antigen-specific pSTAT3-inhibited iTregs or DMSO-treated controls from a healthy donor. The skin-grafted mice were then transplanted with 5 × 10⁶ human PBMCs to induce graft rejection, along with either 1 × 10⁵ pSTAT3-inhibited iTregs or DMSO-treated iTregs, or no iTregs. Thus, the iTregs were autologous to the PBMCs and allogeneic to the skin. The skin grafts were monitored daily for signs of rejection, including ulceration, necrosis, and scabbing (22, 23). Skin grafts that were >75% nonviable were considered rejected. Notably, human skin grafts from mice inoculated with pSTAT3-inhibited iTregs had significantly improved graft survival versus experimental groups treated with vehicle-treated iTregs or PBMCs alone (Figure 2, A and B), and H&E sections from skin grafts on day +21 showed a trend toward reduced rejection pathology within the tissue at this early time point (Figure 2, C and D). Ki-67 staining revealed normal proliferation of basal keratinocytes but highly proliferative, tissue-invasive donor lymphocytes (35) in the dermis of skin grafts from mice receiving control PBMCs or untreated iTregs. In contrast, there were significantly reduced numbers of dermal Ki-67+ cells in the skin grafts from the pSTAT3-inhibited iTreg cohort (Figure 2, E and F). Human pSTAT3–inhibited iTregs also significantly reduced xenogeneic GVHD of the lung, an important target organ in this model (30),
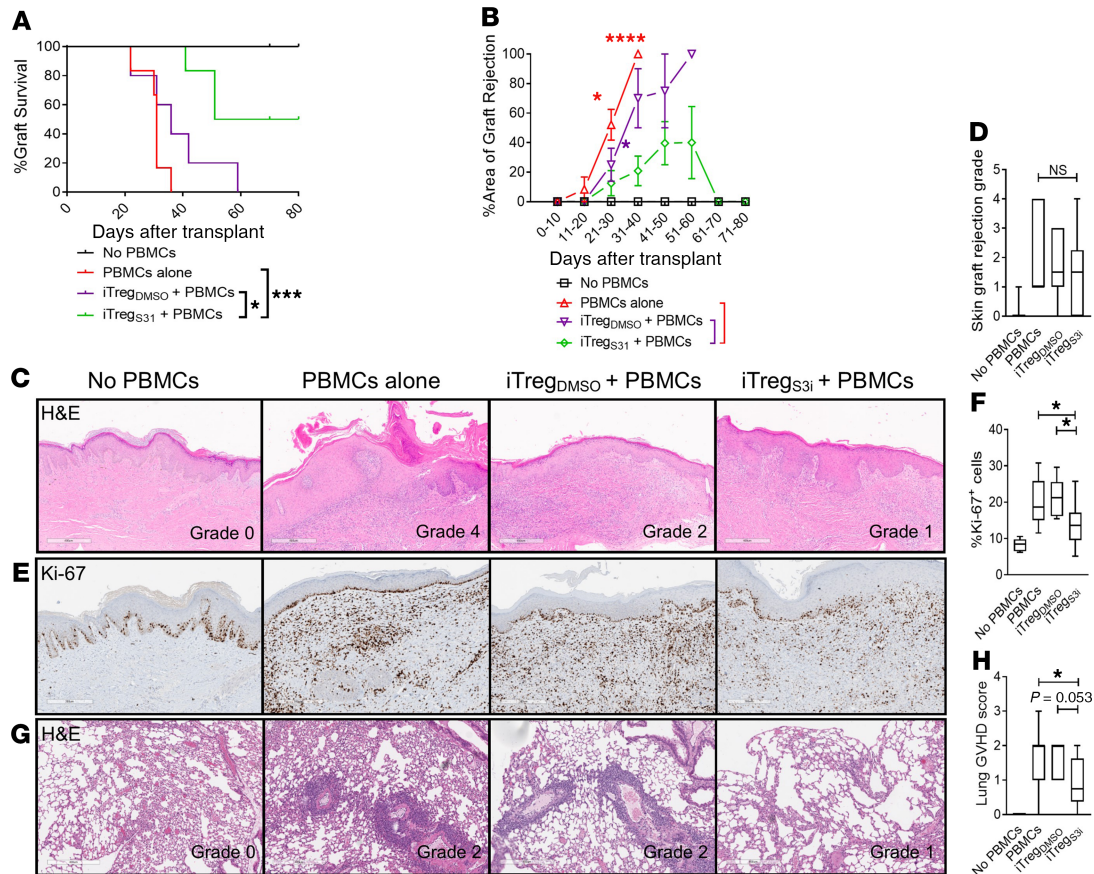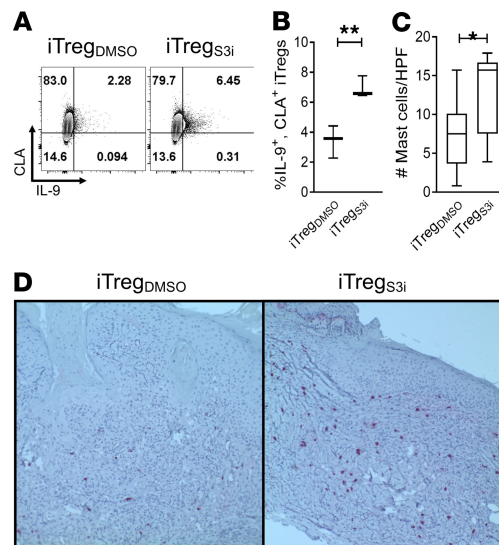
Figure 2. Human pSTAT3–inhibited iTregs significantly reduce skin graft rejection. (A) NSG mice received a 1-cm² human skin graft. Allogeneic pSTAT3-inhibited (S3i) or DMSO-treated iTregs were generated using DCs from the skin donor. After 30 day, the mice received 5×10^6 human PBMCs (autologous to the iTregs and allogeneic to the skin) plus 1×10^5 pSTAT3-inhibited or DMSO-treated iTregs. Graphs shows skin graft (A) survival and (B) Percentage area of graft rejection (mean ± SEM). (C and D) Representative H&E images and graph shows skin graft rejection scores (max, min, median) determined on day +21. (E and F) Ki-67 expression identifies normal proliferating basal keratinocytes and expanding tissue-invasive donor lymphocytes in the dermis of the grafts. Representative IHC images and graph (max, min, median) shows the amount of infiltrating, proliferative, dermal Ki-67⁺ cells in the graft on day +21. (G and H) Representative H&E images and graph (max, min, median) shows the amount of xenogeneic GVHD within the lungs of transplanted NSG mice. $n = 3$ independent experiments with 6–11 mice/group. Log-rank (A) or ANOVA (B, D, F, and H). $*P < 0.05$, $***P = 0.0001$–0.001, $****P < 0.0001$. pSTAT3, STAT3 phosphorylation; iTregs, induced Tregs.

whereas DMSO-treated iTregs were similar to PBMCs alone (Figure 2, G and H). Importantly, human pSTAT3–inhibited iTregs engrafted, expanded in vivo, and clones were detectable by TCR-Vβ sequencing on day +21 (Supplemental Table 1; supplemental material available online with this article; https://doi.org/10.1172/jci.insight.136437DS1).

Human pSTAT3–inhibited iTregs produce ample IL-9 and support cutaneous mast cells. Cutaneous lymphocyte-associated antigen (CLA) is critical for T cells to traffic to the skin, especially in the setting of inflammatory conditions (36). Additionally, IL-9 is an immunosuppressive cytokine produced by Tregs and implicated in tissue tolerance. In particular, IL-9 supports mast cells that provide localized immune suppression and can prevent graft rejection in transplanted rodents (37). Compared with DMSO-treated iTregs, pSTAT3 inhibition significantly increased the frequency of IL-9⁺, CLA⁺ iTregs (Figure 3, A and B). Moreover, NSG mice inoculated with pSTAT3-inhibited iTregs exhibited significantly greater numbers of human mast cells in their skin xenografts (Figure 3, C and D).

Human pSTAT3–inhibited iTregs significantly reduce skin graft infiltration by pathogenic Th2 cells. To assess effects of pSTAT3-inhibited human iTregs on T cells within the graft, NSG mice were transplanted with human skin (22, 23) and then inoculated with allogeneic human PBMCs alone or in combination with pSTAT3-inhibited or vehicle-treated iTregs. On day +21, the mice were humanely euthanized, and the skin grafts were harvested, preserved, and later analyzed by IHC to determine the content of T cell subsets. Human CD4⁺ T cells were significantly reduced in the grafts from mice treated with pSTAT3-inhibited iTregs, compared with
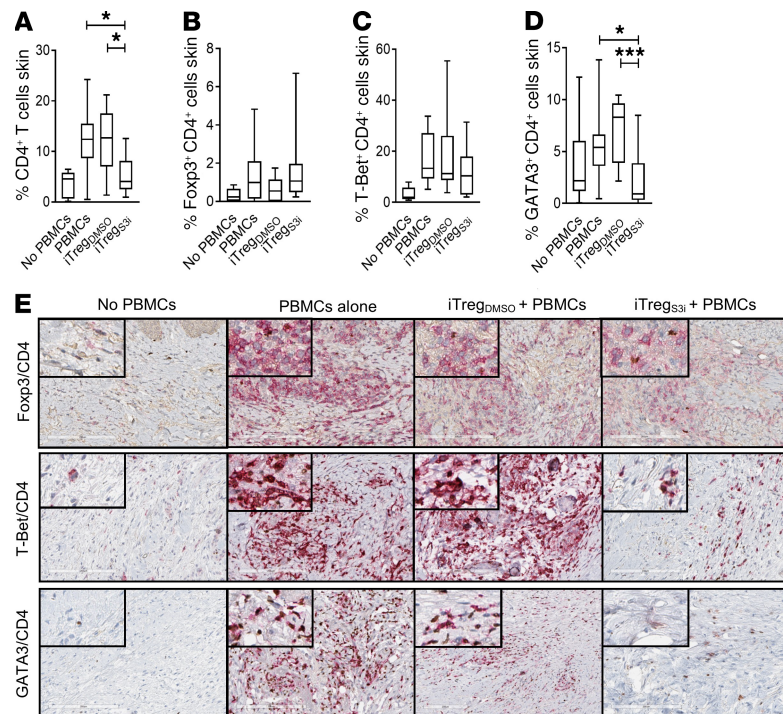
Figure 3. Human pSTAT3–inhibited iTregs produce ample IL-9 and support cutaneous mast cells. pSTAT3-inhibited or DMSO-treated human iTregs were generated as described. (**A**) Contour plots and (**B**) graph (max, min, median) shows the frequency of IL9$^+$, CLA$^+$ CD4$^+$ iTregs after expansion with S3i-201, or DMSO for 5 days from 3 independent experiments. NSG mice received a human skin graft, allogeneic PBMCs, and pSTAT3-inhibited (S3i) or control iTregs. On day +21, the skin grafts were analyzed for mast cell content by tryptase expression using IHC. (**C** and **D**) Graph (max, min, median) and representative images show skin grafts from mice treated with pSTAT3-inhibited iTregs demonstrated significantly more mast cells (tryptase = red). n = 3 independent experiments with 9 mice/group. Paired t test (**B** and **C**). *P < 0.05 or **P = 0.001–0.01. pSTAT3, STAT3 phosphorylation; iTregs, induced Tregs.

PBMCs alone or PBMCs plus DMSO-treated iTregs (Figure 4A). The numbers of Tregs (CD4$^+$, Foxp3$^+$) and Th1 cells (CD4$^+$, T-Bet$^+$) within the skin grafts were similar among mice inoculated with PBMCs alone or in combination with either Treg treatment (Figure 4, B, C, and E). In contrast, numbers of Th2 (CD4$^+$, GATA3$^+$) cells, which are implicated in T cell–mediated inflammatory skin syndromes (38), were significantly reduced in the skin grafts of transplanted mice treated with pSTAT3-inhibited iTregs cells, compared with mice inoculated with PBMCs alone or in combination with vehicle-treated iTregs (Figure 4, D and E).

Human pSTAT3–inhibited iTregs significantly reduce pathogenic Th1 cells in the spleen. To determine the effects of pSTAT3-inhibited iTregs on peripheral T cells beyond the skin grafts, transplanted mice were humanely euthanized on day +21 and human T cells were isolated from the mouse spleens for phenotyping by flow cytometry. The spleens of mice treated with pSTAT3-inhibited iTregs were markedly smaller than mice inoculated with PBMCs alone or with DMSO-treated iTregs (Supplemental Figure 1). Further, total numbers of human CD4$^+$ and CD8$^+$ T cells in the spleen were significantly decreased in mice treated with pSTAT3-inhibited iTregs (Figure 5, A and B). This included proportional reductions in human central memory (CD62L$^+$, CD45RO$^+$), effector memory (CD62L$^-$, CD45RO$^+$), and naive (CD62L$^+$, CD45RO$^-$) T cells residing in the spleen (Figure 5, A and B) (39). Th1 cells (CD4$^+$, IFN-γ$^+$) are implicated in GVHD and allograft rejection (40, 41). Although Th1 cells were unchanged in the skin grafts, the amount of pathogenic Th1 cells was significantly decreased in the spleens of mice treated with pSTAT3-inhibited iTregs, compared with PBMCs alone (Figure 5, C–E). Mice that received DMSO-treated iTregs demonstrated a modest, not statistically significant reduction in Th1 cells, compared with PBMCs alone (Figure 5, C–E).

Unlike the skin grafts, the amount of human Th2 cells (CD4$^+$, IL-4$^+$) in the spleen was similar among all experimental groups (Figure 5, E–G). To gain insights into how pSTAT3-inhibited iTregs influence skin-homing of Th2 cells, we cocultured iTregs with DC-allostimulated T cells. Interestingly, Th2 cells cultured with pSTAT3-inhibited iTregs expressed significantly less CLA (Figure 5, H and I), which is critical for T cell homing to inflamed skin (36). Thus, pSTAT3-inhibited iTregs limit Th2 homing and infiltration of allogeneic skin tissue but permit their differentiation peripherally.

Human pSTAT3–inhibited iTregs reduce the amount of alloreactive Tconv and pathogenic Th17 cells in the periphery. Next, we investigated whether adoptive transfer of pSTAT3-inhibited iTregs affected the amount of Treg or Tconv in the recipient spleens with further flow cytometry analyses. The frequency and absolute number of human splenic Tregs was similar across the experimental groups (Figure 6, A–D).
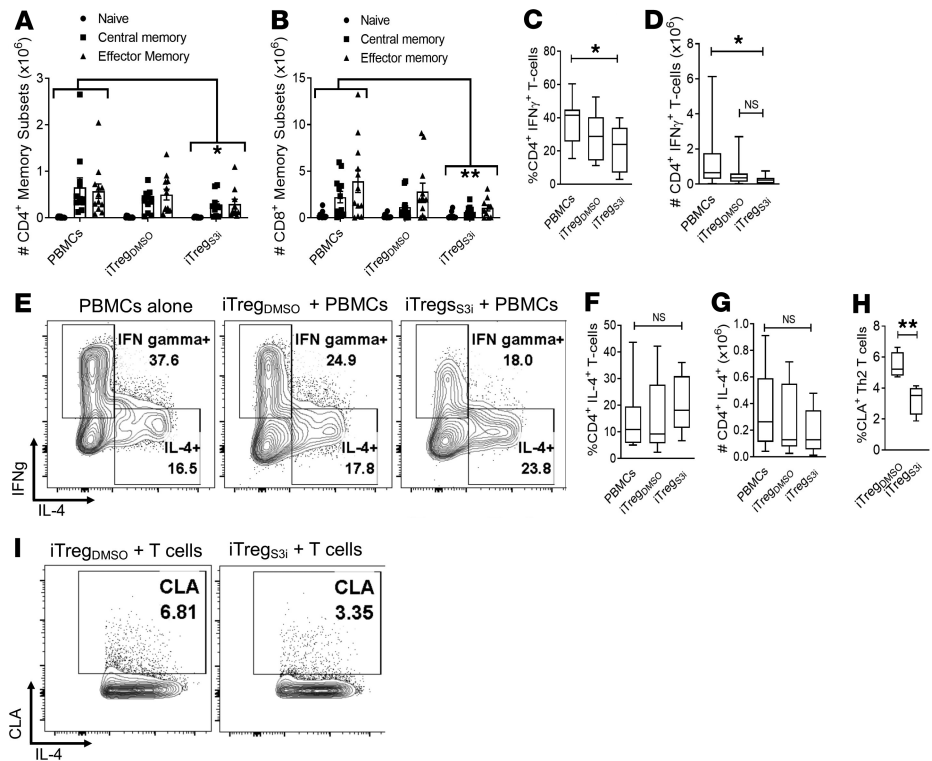
Figure 4. Human pSTAT3–inhibited iTregs significantly reduce skin graft infiltration by pathogenic Th2 cells. NSG mice received a human skin graft, allogeneic PBMCs, and pSTAT3-inhibited (S3i) or control iTregs. On day +21, the skin grafts were analyzed for (**A** and **E**) CD4+ (red), (**B** and **E**) Treg (CD4 red, Foxp3 brown), (**C** and **E**) Th1 (CD4 red, T-Bet brown), and (**D** and **E**) Th2 cells (CD4 red, GATA3 brown). Box-and-whisker plots show max, min, and median. $n = 3$ experiments, up to 11 mice/group. ANOVA (**A–D**). *$P < 0.05$, ***$P = 0.0001-0.001$. pSTAT3, STAT3 phosphorylation; iTregs, induced Tregs.

Although the frequency of human, activated (CD4+, CD127+, CD25+) Tconv in the spleen was similar among the experimental groups, mice treated with pSTAT3-inhibited iTregs demonstrated a significant reduction in the absolute number of activated Tconv (Figure 6, B, E, and F). There was also a trend for increases in the ratio of Treg/activated Tconv among mice treated with pSTAT3-inhibited iTregs (Figure 6G).

Th17 cells can develop from ex-Treg, that is, CD4+ T cells that lose *Foxp3* expression in vivo (42). Moreover, Th17 cells are sufficient to induce GVHD or allograft rejection (40, 43). Importantly, the frequency of human Th17 cells in the spleen was also significantly reduced in mice treated with pSTAT3-inhibited iTregs, versus mice inoculated with PBMCs alone or vehicle-treated iTregs (Figure 7).

Human pSTAT3–inhibited iTregs maintain antileukemia immunity by donor T cells. Using our established method to generate human antitumor cytotoxic T lymphocytes (CTLs) in vivo (22, 23), we tested the effects of pSTAT3-inhibited iTregs on the antileukemia immunity of donor T cells. CTLs were generated in human PBMC–xenotransplanted NSG mice injected with pSTAT3-inhibited iTregs or DMSO-treated iTregs, where an inoculum of irradiated U937 cells was administered on day 0 and day +7. Unvaccinated, xenotransplanted mice served as a negative control. As the iTregs were expanded with skin-donor DCs, the pSTAT3-inhibited iTregs were designed to be antigen-specific and did not inhibit CTL generation or their lytic function against leukemia. Further, CTLs from mice injected with pSTAT3-inhibited or vehicle-treated iTregs were similar in their enhanced killing capacity against U937 targets in vitro, compared with unvaccinated controls (Figure 8). Thus, although antigen-specific, pSTAT3-inhibited iTregs significantly suppress alloreactive T cells and skin graft rejection, they spare donor antileukemia immunity.

Metabolic reprogramming increases the potency of pSTAT3-inhibited iTregs. STAT3 mediates proinflammatory IL-6 receptor signaling and is necessary for optimal electron transport chain (ETC) activity in the mitochondria (44, 45). Foxp3 directs oxidative phosphorylation (OxPhos) in iTregs (46), whereas Tconv prefer glycolysis (44, 47, 48). Others have demonstrated that Tregs that utilize glycolysis and exhibit reduced OxPhos are dysfunctional (49). Notably, pSTAT3 inhibition in iTregs compromised OxPhos (Figure 9A)
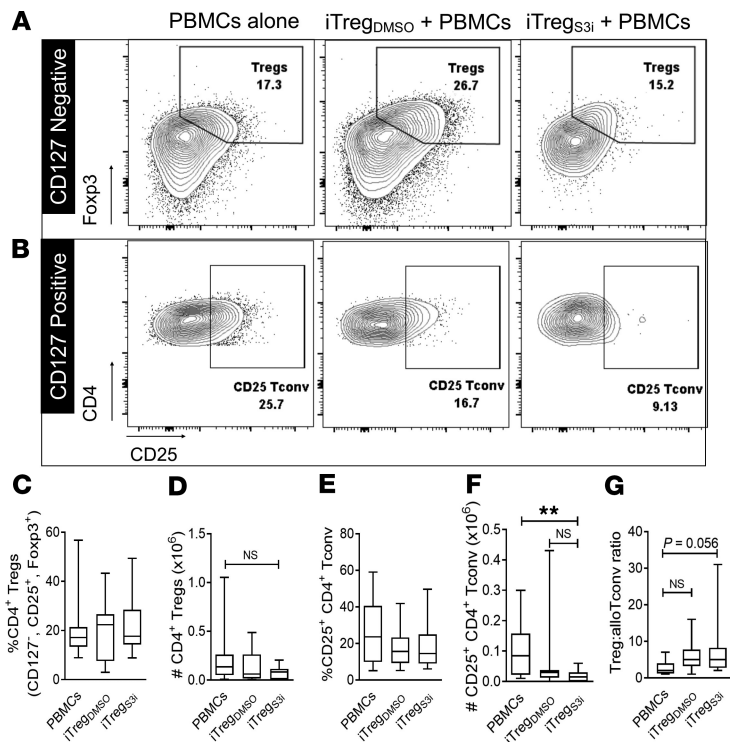
Figure 5. Human pSTAT3–inhibited iTregs significantly reduce pathogenic Th1 cells in the spleen. NSG mice received a human skin graft, allogeneic PBMCs, and pSTAT3-inhibited (S3i) or control iTregs. On day +21, the recipient spleens were harvested and analyzed for human T cell numbers and effector subsets. Graphs show the absolute numbers of (**A**) CD4$^+$ and (**B**) CD8$^+$ central memory (CD62L$^+$, CD45RO$^+$), effector memory (CD62L$^-$, CD45RO$^+$), and naive T cells (CD62L$^+$, CD45RO$^-$) ± SEM. (**C–G**) Box and-whisker plots (max, min, median) show the frequency and absolute number of human Th1 (CD4$^+$, IFN-γ^+) and Th2 cells (CD4$^+$, IL-4$^+$), with representative contour plots showing the T cell populations. n = 3 experiments, up to 11 mice/group. Human pSTAT3–inhibited or DMSO-treated iTregs were cultures with autologous CD4$^+$ T cells with allogeneic DCs (T cell to DC ratio 30:1) for 5 days. The frequency of skin-homing CLA expression (**H**) on the CD4$^+$, IL-4$^+$ (max, min, median) was determined by flow cytometry. (**I**) Representative contour plots are shown. n = 4 independent experiments. ANOVA (**A–D**, **F**, and **G**) or paired t test (**H**). *$P < 0.05$ or **$P = 0.001–0.01$. pSTAT3, STAT3 phosphorylation; iTregs, induced Tregs.

and induced a shift toward glycolysis (Figure 9B). To test if this detrimental effect on OxPhos by pSTAT3 inhibition could be overcome, we generated iTregs with S3i-201 and CoQ10, as CoQ10 can replace electron deficiencies by directly stimulating complex II of the ETC (50). These studies revealed that CoQ10 treatment elevated basal and restores the maximal spare capacity for OxPhos in pSTAT3-inhibited iTregs (Figure 9A), and significantly decreased glycolysis (Figure 9B). Notably, CoQ10 treatment further augmented the suppressive potency of pSTAT3-inhibited iTregs in vitro (Figure 9C). Finally, in the human skin/NSG mouse xenograft model, pSTAT3-inhibited iTregs treated with CoQ10 augmented protection from alloreactive T cells in vivo, whereas human iTregs generated with S3i-201 and CoQ10 were superior at reducing skin graft rejection compared with pSTAT3 inhibition alone (Figure 9, D and E). Indeed, rescuing OxPhos in pSTAT3-inhibited iTregs by ex vivo treatment with CoQ10 optimized their suppressive potency, where 90% of the transplanted mice were free of graft rejection (Figure 9D).

Discussion

Here we demonstrate that adoptive transfer of human pSTAT3–inhibited iTregs prevents skin graft rejection and xenogeneic GVHD by donor T cells. Therefore, adoptive transfer of pSTAT3-inhibited iTregs could benefit recipients of solid-organ allografts or alloHCT alike, to prevent graft rejection or GVHD, respectively. Mechanistically, pSTAT3 inhibition in iTregs augments demethylation of the *FOXP3* TSDR and Foxp3 expression, stabilizing their suppressive phenotypic (21), and here we show this is associated with increased expression of the immune checkpoints GARP and PD-1 that are important for the enhanced potency of the pSTAT3-inhibited iTregs. Importantly, our current study offers preclinical proof-of-concept evidence
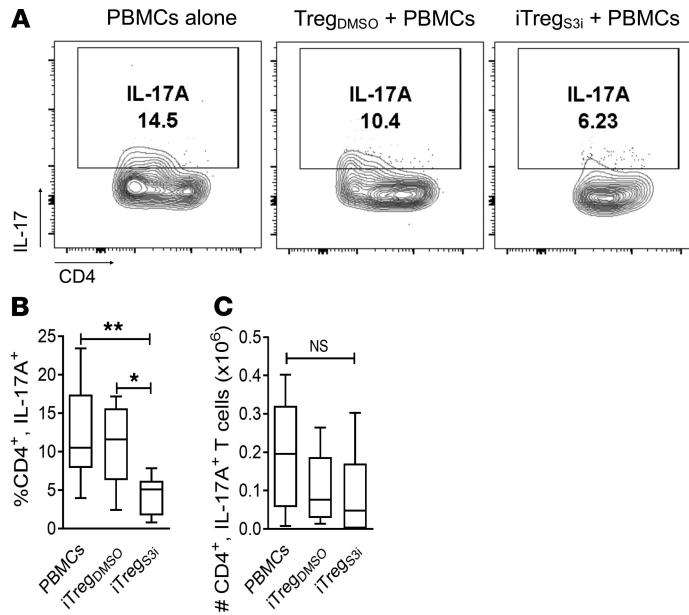
Figure 6. Human pSTAT3–inhibited iTregs reduce the amount of alloreactive Tconv. NSG mice received a human skin graft, allogeneic PBMCs, and pSTAT3-inhibited (S3i) or control iTregs. On day +21, the recipient spleens were harvested and analyzed for human Treg (CD4$^+$, CD127$^-$, CD25$^+$, Foxp3$^+$) and activated Tconv (CD4$^+$, CD127$^+$, CD25$^+$). (**A** and **B**) Representative contour plots are shown. Box-and-whisker plots (max, min, median) demonstrate the frequency and absolute numbers of human Tregs (**C** and **D**) and activated Tconv (**E** and **F**). (**G**) Graph (max, min, median) shows the ratio of Treg to activated Tconv within the recipient spleens on day +21. n = 3 experiments, up to 11 mice/group. ANOVA (**C–G**). *P < 0.05. pSTAT3, STAT3 phosphorylation; iTregs, induced Tregs; Tconv, conventional T cells.

that pSTAT3-inhibited iTregs (a) have superior suppression over alloreactive human T cells in vivo; (b) limit tissue invasion by pathogenic Th2 cells into skin, a highly antigenic tissue and common GVHD target organ; (c) recruit immunosuppressive mast cells via IL-9; (d) significantly reduce alloreactive Tconv, Th1, and Th17 cells in the periphery; and (e) preserve donor antileukemia activity, a key benefit of alloHCT. Moreover, the infused human pSTAT3–inhibited iTregs persist and expand in vivo.

Increased IL-6 responsiveness and STAT3 phosphorylation in CD4$^+$ T cells is associated with high rates of grade II–IV acute GVHD (16, 51). STAT3 competes with STAT5 for access to *FOXP3* promoters and antagonizes Treg development (52, 53). We previously attempted to enhance Treg expansion and peripheral induction early after alloHCT by polarizing pSTAT5 signaling in circulating CD4$^+$ T cells in our phase II GVHD prevention trial of low-dose IL-2 (16). In that study, we achieved a significant, but temporary, increase in Treg reconstitution (16). Specifically, although IL-2 improved pSTAT5 activity in donor CD4$^+$ T cells, this regimen failed to mitigate aberrant pSTAT3 activation in the same cells, and most patients that developed grade II-IV acute GVHD exhibited high numbers of circulating pSTAT3$^+$CD4$^+$ T cells (16). Systemic pSTAT3 inhibition is, however, translationally challenging because current small molecule inhibitors are limited by toxicity (54). Thus, we hypothesized that directly inhibiting STAT3 phosphorylation during the generation of iTreg ex vivo, followed by their adoptive transfer to transplant recipients, could significantly suppress alloreactive T cells and reduce GVHD.

Although several GVHD prevention trials using peripheral or "natural" Tregs have been conducted (2, 12, 18), very few have tested iTregs for the same indication (55). In solid-organ transplantation, early phase trials are currently underway to investigate the safety and preliminary efficacy of human peripheral, but not induced, Tregs in allograft rejection prophylaxis (17). From a translational perspective, iTregs offer an advantage over peripheral Tregs because they come from a large and readily available pool of CD4$^+$ Tconv, compared with an otherwise rare population of peripheral Tregs. Thus, iTregs are amenable to efficient clinical scale production. However, iTregs suffer from phenotypic instability

A

PBMCs alone | Treg$_{DMSO}$ + PBMCs | iTreg$_{S3i}$ + PBMCs

Figure 7. The amount of human Th17 cells is reduced in mice treated with pSTAT3-inhibited iTregs. NSG mice received a human skin graft, allogeneic PBMCs, and pSTAT3-inhibited (S3i) or control iTregs. On day +21, the recipient spleens were harvested and analyzed for human Th17 cells (CD4$^+$, IL-17A$^+$). Representative contour plots (**A**) and graphs (max, min, median) show the frequency (**B**) and absolute number (**C**) of human Th17 cells within the recipient spleens on day +21. n = 3 experiments, up to 11 mice/group. ANOVA (**B** and **C**). *P < 0.05 or **P = 0.001–0.01. pSTAT3, STAT3 phosphorylation; iTregs, induced Tregs.

and can revert to potentially inflammatory Tconv (56). Likely given this plasticity, adoptive transfer of iTregs for GVHD prevention in preclinical models has shown mixed efficacy, where human iTregs showed efficacy in reducing xenogeneic GVHD (57), but murine iTregs failed to prevent GVHD (56). Further, in a phase I trial, human iTregs have safely been administered as GVHD prophylaxis, yet the trial was not powered to test efficacy and did not appear to significantly reduce GVHD (55). Similarly, in our preclinical xenogeneic NSG model, vehicle-treated iTregs failed to protect recipients against human skin graft rejection, yet, importantly, they did not accelerate rejection or xenogeneic GVHD. In contrast and importantly, we have shown that inhibiting pSTAT3 optimizes iTreg suppressive functions to overcome tissue rejection by alloreactive human T cells.

Though pSTAT3 inhibition enhances iTreg potency and stabilizes its suppressive phenotype, mitochondrial STAT3 is necessary for optimal activity of the ETC (44, 45). In accord with these studies, here we show that pSTAT3 inhibition compromises OxPhos in iTregs and provokes a shift toward glycolysis. Given these findings, we reasoned that although pSTAT3-inhibited iTregs significantly reduce alloreactive T cells, impaired OxPhos might limit iTreg fitness and long-term durability. Indeed, we showed that treatment with CoQ10, which is accepted by complex II of the ETC and facilitates OxPhos by shuttling electrons to complex III in the mitochondria (50), rescues OxPhos in pSTAT3-inhibited iTregs, and further augments their suppressive potency against alloreactive T cells both in vitro and in vivo. In contrast, adding CoQ10 to vehicle-treated iTregs further improved OxPhos but did not affect their suppressive function. We conclude that increased OxPhos alone is insufficient to enhance iTreg potency and that other targets affected by pSTAT3 inhibition also contribute to the superior suppressive responses of these iTregs (e.g., PD-1 and GARP). Our findings are consistent with those of the Chi Lab and others (49), in

Figure 8. Human pSTAT3–inhibited iTregs maintain antileukemia immunity by donor T cells. Graph depicts mean lysis ± SEM by U937-specific, human T cells generated in vivo using NSG mice transplanted with human PBMCs, pSTAT3-inhibited (S3i) or control iTregs, and then vaccinated with irradiated U937cells (2 × 10⁶, ATCC) on days 0 and +7. Human T cells from nonvaccinated mice containing PBMCs alone group served as a negative control. On day +12, the mice were euthanized, and human T cells were harvested and purified from the spleen using magnetic bead separation. Tregs were specifically not removed from the harvested T cells. The purified T cells were cultured with fresh U937 targets at varying ratios. U937 lysis was measured using a colorimetric assay after 4 hours of culture. Results shown are from 1 of 2 independent experiments, using 4 mice per group. ANOVA. ****P < 0.0001. pSTAT3, STAT3 phosphorylation; iTregs, induced Tregs.
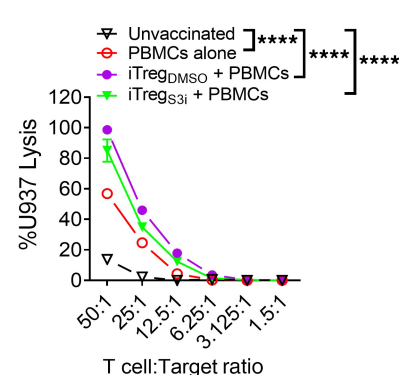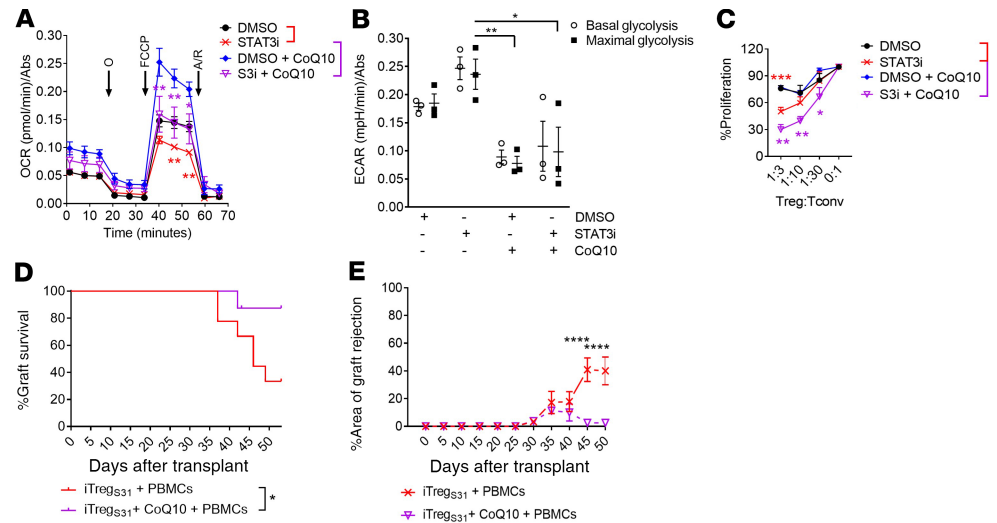
Figure 9. pSTAT3-inhibited iTregs increase their potency after metabolic reprogramming. Human iTregs were generated with allogeneic DCs while exposed to S3i-201 or DMSO for 5 days and purified by CD25 magnetic bead isolation, then the (**A**) oxygen consumption rate (OCR) and (**B**) extracellular acidification rate (ECAR) were evaluated using a Seahorse XF Analyzer. Where indicated CoQ10 (10ng/ml) or PBS was added to the iTreg culture to rescue OxPhos. In all cases, the medium was supplemented with IL-2 during iTreg expansion. As OxPhos was improved by adding CoQ10 to pSTAT3-inhibited iTregs, we then tested its effect on iTreg function. (**C**) Graph shows the suppressive activity (mean ± SEM) of pSTAT3-inhibited or control iTregs, treated with or without CoQ10, against alloreactive T cells. $n = 4$ independent experiments. NSG mice received a human skin graft, 5×10^6 allogeneic PBMCs, and 1×10^5 pSTAT3-inhibited (S3i) treated with or without CoQ10 during culture. Graphs show skin graft (**D**) survival and (**E**) Percentage area of graft rejection (mean ± SEM). $n = 2$ independent experiments with up to 9 mice/group. ANOVA (**A–C**, and **E**) or log-rank (**D**). *$P < 0.05$, **$P = 0.001–0.01$, ***$P = 0.0001–0.001$, and ****$P < 0.0001$. pSTAT3, STAT3 phosphorylation; iTregs, induced Tregs; CoQ10, coenzyme Q10; OxPhos, oxidative phosphorylation.

which Tregs that use glycolysis over OxPhos exhibit limited suppressive function. However, it is important to note that glycolysis is possibly beneficial in other aspects of Treg biology, such as migration (58) and differentiation (59). Although we investigated the effects of pSTAT3 inhibition on iTreg metabolism, it is also possible that S3I-201 and/or CoQ10 may have important biologic effects beyond those identified in the present study.

Adoptive transfer of metabolically tuned, pSTAT3-inhibited iTregs is a readily translatable strategy to prevent GVHD or graft rejection mediated by alloreactive human T cells. Moreover, pSTAT3-inhibited iTregs preserve donor antileukemia activity necessary for the beneficial graft-versus-leukemia effect. Despite recent FDA approvals for agents to treat steroid refractory acute (60) and chronic GVHD (61), advances in GVHD prevention are needed. Additionally, innovative approaches are needed in solid-organ allotransplantation to reduce dependence on broadly suppressive calcineurin inhibitors and glucocorticoids. Thus, we are actively scaling up production of these iTregs to clinically test in GVHD prophylaxis. We predict that pSTAT3 inhibition combined with effective metabolic reprogramming by CoQ10 will provide highly effective CD4+ iTreg-based GVHD prophylaxis and submit that this strategy warrants full clinical investigation.

Methods

Monoclonal antibodies and flow cytometry. Fluorochrome-conjugated mouse anti–human monoclonal antibodies included anti-CD3, CD4, CD25, CD45RO, CD62L, CD127, GARP, PD-1, CD39, LAG3, CTLA4, IL-9, CLA, Foxp3, Ki-67, IFN-γ, IL-17A, and IL-4 (BD Biosciences; Cell Signaling Technology) (Supplemental Table 2). LIVE/DEAD Fixable Yellow or Aqua Dead Cell Stain (Life Technologies) was used to determine viability. Live events were acquired on a BD FACSCanto II or LSRII flow cytometer (FlowJo software, ver. 7.6.4; TreeStar).

Treg generation and functional experiments. Tregs were defined as CD4+, CD127−, CD25+, and Foxp3+ cells (28, 29). Induced Tregs were generated by stimulating purified CD4+, CD25- T cells with allogeneic monocyte-derived DCs (T cell to DC ratio = 30:1) for 5 days in the presence of pSTAT3 inhibitor, S3i-201

(50 μM), or DMSO (0.1%) for 5 days in medium supplemented with recombinant human IL-2 (20 IU/ml) as published (21). Where indicated, iTregs were generated with CD3/CD28 stimulator beads. In select experiments, STAT3 siRNA (Dharmacon Accell) was used to knock down STAT3 molecularly. Treg potency was determined using our standard suppression assay (26). S3i-201 or DMSO was added to the initial culture only to expand the Tregs. No drug was added to the suppression assay medium. Conventional, alloreactive T cell (Tconv) proliferation was measured by Ki-67 expression using flow cytometry. Where indicated, anti–human LAP/TGF-β1 (ligand of GARP) (31, 32) mAb, anti–human PD-1 (10 μg/ml) mAb, CD39 ectonucleotidase inhibitor (ARL67156, 125 μM) (30), or control (PBS plus isotype) was added to the suppression assay medium to neutralize GARP, PD-1, or CD39 activity, respectively.

Xenograft model and in vivo CTL generation. NSG mice received a 1-cm^2, split-thickness human skin graft (22, 23). The skin grafts were allowed to heal and facilitate engraftment. During this time, human monocyte-derived DCs (moDCs) were generated from blood autologous to the skin graft donor using GmCSF and IL-4, then matured with a standardized combination of inflammatory cytokines and prostaglandin E2 (PGE2) as described (21, 62). These moDCs were then used to generate and expand allogeneic pSTAT3-inhibited iTregs or vehicle-treated iTregs from a healthy donor (OneBlood or Memorial Blood Centers), using S3i-201 (21, 27, 51) or DMSO, respectively. In select experiments, the iTregs were supplemented with CoQ10 (10 ng/ml) during culture. The skin-grafted mice were then transplanted with 5×10^6 human PBMCs to induce graft rejection, along with either 1×10^5 pSTAT3-inhibited iTregs or vehicle-treated iTregs, or no iTregs (note that the iTregs were autologous to the PBMCs, and allogeneic to the skin). The skin grafts were then monitored daily for signs of rejection, including ulceration, necrosis, and scabbing (22, 23). Skin grafts that were >75% nonviable were considered rejected.

In select experiments, mice were humanely euthanized on day +21; skin grafts and host spleens were harvested for analysis. Skin rejection was performed blinded according to standard criteria (26, 33, 38). Processed spleens cells were phenotyped by flow cytometry for Tregs, Tconv, Th1, Th2, and Th17 cells (22, 23, 30). IHC was performed on the skin grafts to identify Tregs (CD4 and Foxp3), Th1 (CD4 and T-bet), and Th2 (CD4 and GATA3) and scanned by use of ScanScope XT (Aperio Technologies) with a 200×/0.75 NA objective lens at a rate of 3 minutes per slide via Basler Tri-linear array as described (51). In addition, Ki-67 staining was conducted to identify proliferative, infiltrative lymphocytes in the dermis and tryptase staining was performed to characterize mast cell content in the grafts.

To test the effect of pSTAT3-inhibited iTreg effects on the donor T cell–mediated response against U937 leukemia cells, mice were transplanted with 5×10^6 human PBMCs, with or without pSTAT3-inhibited or DMSO-treated iTregs (1×10^5) and received an inoculum of irradiated U937 cells (2×10^6) on day 0 and +7 (22, 23). Control mice received PBMCs alone without tumor. Mice did not receive skin grafts for these experiments. On day +12, the mice were humanely euthanized, and the spleens were harvested. Human CD3$^+$ T cells within the spleens were purified by magnetic beads. Tregs were specifically not removed from the harvested T cells. The human T cells were cocultured with fresh U937 cells at varying T cell to Target ratios for 4 hours. Tumor lysis assays were performed in vitro using a colorimetric assay (22, 23).

Metabolism experiments. Pretreated, purified pSTAT3-inhibited or DMSO-treated iTregs (2×10^5) were washed once and then plated in XFe96 microplates in unbuffered DMEM containing 10 mM glucose, 1 mM sodium pyruvate, and 2 mM L-glutamine for mitochondrial stress test assays or unbuffered DMEM only for the glycolytic stress test assays. The concentration of the compounds used were as follows: 1 μM oligomycin A, 1 μM FCCP, 500 nM rotenone, 500 nM antimycin A, 10 mM glucose, and 1 mM 2-DG. Data were normalized using Calcein AM.

Statistics. One-way ANOVA was used for group comparisons, including a Sidak's or Dunn's post test for correction of multiple comparisons. A paired *t* test was used for paired comparisons. For comparison of survival curves, a log-rank test was used. The statistical analysis was conducted using Prism software version 5.04 (GraphPad). Statistical significance was defined by a 2-tailed $P < 0.05$.

Study approval. Skin and peripheral blood mononuclear cells were acquired from consented mastectomy patients using an IRB-approved protocol at Moffitt Cancer Center and the University of Minnesota Masonic Cancer Center. NSG mice (male or female, age 6- to 24-weeks-old) were purchased from The Jackson Laboratory and housed within American Association for Laboratory Animal Care–accredited Animal Resource Centers at Moffitt Cancer Center or the University of Minnesota. All mice were treated in adherence with the NIH *Guide for the Care and Use of Laboratory Animals* (National Academies Press, 2011), and the protocols used were approved by the Moffitt Cancer Center or the University of Minnesota institutional animal care and use committees.

Author contributions

KW performed experiments, analyzed and interpreted data, and edited the manuscript. MRF performed and analyzed experiments and edited the manuscript. JR performed experiments. JK designed experiments and provided statistical expertise. MCL, JVK, and JH consented patients and acquired human skin grafts. EMS, MAL, MH, and CF performed histologic and pathologic analyses of xenograft data and edited the manuscript. NJL, HRL, and SMS synthesized S3i-201 and edited the manuscript. JP, SZP, DM Jr, JLC, BRB, and CA assisted in the design of experiments and edited the manuscript. BCB designed, led, and performed experiments, analyzed and interpreted data, and wrote the manuscript.

Address correspondence to: Brian C. Betts, Nils Hasselmo Hall, Room 2-108, 312 Church Street SE, Minneapolis, Minnesota 55455, USA. Phone: 612.625.8942; Email: Bett0121@umn.edu.

1. Brunstein CG, et al. Infusion of ex vivo expanded T regulatory cells in adults transplanted with umbilical cord blood: safety profile and detection kinetics. *Blood*. 2011;117(3):1061–1070.

2. Veerapathran A, et al. CD4 Treg and CD4 Tcon utilize distinct TCR Vβ repertoires in response to alloantigen. *Blood*. 2015;126(23):4286.

3. Anderson A, et al. Expanded nonhuman primate tregs exhibit a unique gene expression signature and potently downregulate alloimmune responses. *Am J Transplant*. 2008;8(11):2252–2264.

4. McDonald-Hyman C, et al. Therapeutic regulatory T-cell adoptive transfer ameliorates established murine chronic GVHD in a CXCR5-dependent manner. *Blood*. 2016;128(7):1013–1017.

5. Martin-Moreno PL, Tripathi S, Chandraker A. Regulatory T cells and kidney transplantation. *Clin J Am Soc Nephrol*. 2018;13(11):1760–1764.

6. Vaeth M, et al. Selective NFAT targeting in T cells ameliorates GvHD while maintaining antitumor activity. *Proc Natl Acad Sci U S A*. 2015;112(4):1125–1130.

7. Singh K, et al. Superiority of rapamycin over tacrolimus in preserving nonhuman primate Treg half-life and phenotype after adoptive transfer. *Am J Transplant*. 2014;14(12):2691–2703.

8. Zeiser R, et al. Inhibition of CD4+CD25+ regulatory T-cell function by calcineurin-dependent interleukin-2 production. *Blood*. 2006;108(1):390–399.

9. Cutler C, et al. Tacrolimus/sirolimus vs tacrolimus/methotrexate as GVHD prophylaxis after matched, related donor allogeneic HCT. *Blood*. 2014;124(8):1372–1377.

10. Pidala J, et al. A randomized phase II study to evaluate tacrolimus in combination with sirolimus or methotrexate after allogeneic hematopoietic cell transplantation. *Haematologica*. 2012;97(12):1882–1889.

11. Ekberg H, et al. Reduced exposure to calcineurin inhibitors in renal transplantation. *N Engl J Med*. 2007;357(25):2562–2575.

12. Brunstein CG, et al. Umbilical cord blood-derived T regulatory cells to prevent GVHD: kinetics, toxicity profile, and clinical effect. *Blood*. 2016;127(8):1044–1051.

13. Pidala J, et al. Prolonged sirolimus administration after allogeneic hematopoietic cell transplantation is associated with decreased risk for moderate-severe chronic graft-versus-host disease. *Haematologica*. 2015;100(7):970–977.

14. Gooptu M, et al. Effect of sirolimus on immune reconstitution following myeloablative allogeneic stem cell transplantation: an ancillary analysis of a randomized controlled trial comparing tacrolimus/sirolimus and tacrolimus/methotrexate (Blood and Marrow Transplant Clinical Trials Network/BMT CTN 0402). *Biol Blood Marrow Transplant*. 2019;25(11):2143–2151.

15. Kennedy-Nasser AA, et al. Ultra low-dose IL-2 for GVHD prophylaxis after allogeneic hematopoietic stem cell transplantation mediates expansion of regulatory T cells without diminishing antiviral and antileukemic activity. *Clin Cancer Res*. 2014;20(8):2215–2225.

16. Betts BC, et al. IL-2 promotes early Treg reconstitution after allogeneic hematopoietic cell transplantation. *Haematologica*. 2017;102(5):948–957.

17. Tang Q, Vincenti F. Transplant trials with Tregs: perils and promises. *J Clin Invest*. 2017;127(7):2505–2512.

18. Kellner JN, et al. Third party, umbilical cord blood derived regulatory T-cells for prevention of graft versus host disease in allogeneic hematopoietic stem cell transplantation: feasibility, safety and immune reconstitution. *Oncotarget*. 2018;9(86):35611–35622.

19. Veerapathran A, et al. Human regulatory T cells against minor histocompatibility antigens: ex vivo expansion for prevention of graft-versus-host disease. *Blood*. 2013;122(13):2251–2261.

20. Williams LM, Rudensky AY. Maintenance of the Foxp3-dependent developmental program in mature regulatory T cells requires continued expression of Foxp3. *Nat Immunol*. 2007;8(3):277–284.

21. Betts BC, Veerapathran A, Pidala J, Yu XZ, Anasetti C. STAT5 polarization promotes iTregs and suppresses human T-cell allo-responses while preserving CTL capacity. *J Leukoc Biol*. 2014;95(2):205–213.

22. Betts BC, et al. Targeting JAK2 reduces GVHD and xenograft rejection through regulation of T cell differentiation. *Proc Natl Acad Sci U S A*. 2018;115(7):1582–1587.

23. Betts BC, et al. Inhibition of human dendritic cell ER stress response reduces T cell alloreactivity yet spares donor anti-tumor immunity. *Front Immunol*. 2018;9:2887.

24. Steinmuller D. Skin allograft rejection by stable hematopoietic chimeras that accept organ allografts sill is an enigma. *Transplantation*. 2001;72(1):8–9.

25. Boyse EA, Old LJ. Loss of skin allograft tolerance by chimeras. *Transplantation*. 1968;6(4):619.

26. Moseley RV, Sheil AG, Mitchell RM, Murray JE. Immunologic relationships between skin and kidney homografts in dogs on immunosuppressive therapy. *Transplantation*. 1966;4(6):678–687.

27. Siddiquee K, et al. Selective chemical probe inhibitor of Stat3, identified through structure-based virtual screening, induces anti-tumor activity. *Proc Natl Acad Sci U S A*. 2007;104(18):7391–7396.

28. Liu W, et al. CD127 expression inversely correlates with FoxP3 and suppressive function of human CD4+ T reg cells. *J Exp Med*. 2006;203(7):1701–1711.

29. Seddiki N, et al. Expression of interleukin (IL)-2 and IL-7 receptors discriminates between human regulatory and activated T cells. *J Exp Med*. 2006;203(7):1693–1700.

30. Betts BC, et al. Targeting Aurora kinase A and JAK2 prevents GVHD while maintaining Treg and antitumor CTL function. *Sci Transl Med*. 2017;9(372):eaai8269.

31. Hahn SA, et al. A key role of GARP in the immune suppressive tumor microenvironment. *Oncotarget*. 2016;7(28):42996–43009.

32. Hahn SA, et al. Soluble GARP has potent antiinflammatory and immunomodulatory impact on human CD4+ T cells. *Blood*. 2013;122(7):1182–1191.

33. Young JW, Merad M, Hart DN. Dendritic cells in transplantation and immune-based therapies. *Biol Blood Marrow Transplant*. 2007;13(1 suppl 1):23–32.

34. Paczesny S, et al. Elafin is a biomarker of graft-versus-host disease of the skin. *Sci Transl Med*. 2010;2(13):13ra2.

35. Sagoo P, Ali N, Garg G, Nestle FO, Lechler RI, Lombardi G. Human regulatory T cells with alloantigen specificity are more potent inhibitors of alloimmune skin graft damage than polyclonal regulatory T cells. *Sci Transl Med*. 2011;3(83):83ra42.

36. Colantonio L, Iellem A, Sinigaglia F, D'Ambrosio D. Skin-homing CLA+ T cells and regulatory CD25+ T cells represent major subsets of human peripheral blood memory T cells migrating in response to CCL1/I-309. *Eur J Immunol*. 2002;32(12):3506–3514.

37. Lu LF, et al. Mast cells are essential intermediaries in regulatory T-cell tolerance. *Nature*. 2006;442(7106):997–1002.

38. Laffont S, et al. CD8+ T-cell-mediated killing of donor dendritic cells prevents alloreactive T helper type-2 responses in vivo. *Blood*. 2006;108(7):2257–2264.

39. Seder RA, Darrah PA, Roederer M. T-cell quality in memory and protection: implications for vaccine design. *Nat Rev Immunol*. 2008;8(4):247–258.

40. Zelenika D, et al. Rejection of H-Y disparate skin grafts by monospecific CD4+ Th1 and Th2 cells: no requirement for CD8+ T cells or B cells. *J Immunol*. 1998;161(4):1868–1874.

41. Yu Y, et al. Prevention of GVHD while sparing GVL effect by targeting Th1 and Th17 transcription factor T-bet and RORγt in mice. *Blood*. 2011;118(18):5011–5020.

42. Komatsu N, et al. Pathogenic conversion of Foxp3+ T cells into TH17 cells in autoimmune arthritis. *Nat Med*. 2014;20(1):62–68.

43. Iclozan C, et al. T helper17 cells are sufficient but not necessary to induce acute graft-versus-host disease. *Biol Blood Marrow Transplant*. 2010;16(2):170–178.

44. Angelin A, et al. Foxp3 reprograms T cell metabolism to function in low-glucose, high-lactate environments. *Cell Metab*. 2017;25(6):1282–1293.e7.

45. Wegrzyn J, et al. Function of mitochondrial Stat3 in cellular respiration. *Science*. 2009;323(5915):793–797.

46. Howie D, et al. Foxp3 drives oxidative phosphorylation and protection from lipotoxicity. *JCI Insight*. 2017;2(3):e89160.

47. Pacella I, et al. Fatty acid metabolism complements glycolysis in the selective regulatory T cell expansion during tumor growth. *Proc Natl Acad Sci U S A*. 2018;115(28):E6546–E6555.

48. Gerriets VA, et al. Foxp3 and Toll-like receptor signaling balance T_{reg} cell anabolic metabolism for suppression. *Nat Immunol*. 2016;17(12):1459–1466.

49. Wei J, et al. Autophagy enforces functional integrity of regulatory T cells by coupling environmental cues and metabolic homeostasis. *Nat Immunol*. 2016;17(3):277–285.

50. Echtay KS, Winkler E, Klingenberg M. Coenzyme Q is an obligatory cofactor for uncoupling protein function. *Nature*. 2000;408(6812):609–613.

51. Betts BC, et al. CD4+ T cell STAT3 phosphorylation precedes acute GVHD, and subsequent Th17 tissue invasion correlates with GVHD severity and therapeutic response. *J Leukoc Biol*. 2015;97(4):807–819.

52. Laurence A, et al. Interleukin-2 signaling via STAT5 constrains T helper 17 cell generation. *Immunity*. 2007;26(3):371–381.

53. Yao Z, et al. Nonredundant roles for Stat5a/b in directly regulating Foxp3. *Blood*. 2007;109(10):4368–4375.

54. Lu SX, et al. STAT-3 and ERK 1/2 phosphorylation are critical for T-cell alloactivation and graft-versus-host disease. *Blood*. 2008;112(13):5254–5258.

55. MacMillan ML, et al. First-in-human clinical trial to determine the safety and potency of inducible t regulatory cells after allogeneic hematopoietic cell transplantation. *Blood*. 2018;132(supp_l1):2112.

56. Beres A, Komorowski R, Mihara M, Drobyski WR. Instability of Foxp3 expression limits the ability of induced regulatory T cells to mitigate graft versus host disease. *Clin Cancer Res*. 2011;17(12):3969–3983.

57. Hippen KL, et al. In vitro induction of human regulatory T cells using conditions of low tryptophan plus kynurenines. *Am J Transplant*. 2017;17(12):3098–3113.

58. Kishore M, et al. Regulatory T cell migration is dependent on glucokinase-mediated glycolysis. *Immunity*. 2017;47(5):875–889.e10.
59. De Rosa V, et al. Glycolysis controls the induction of human regulatory T cells by modulating the expression of FOXP3 exon 2 splicing variants. *Nat Immunol*. 2015;16(11):1174–1184.
60. Przepiorka D, et al. FDA Approval Summary: ruxolitinib for treatment of steroid-refractory acute graft-versus-host disease. *Oncologist*. 2020;25(2):e328–e334.
61. Jaglowski SM, Blazar BR. How ibrutinib, a B-cell malignancy drug, became an FDA-approved second-line therapy for steroid-resistant chronic GVHD. *Blood Adv*. 2018;2(15):2012–2019.
62. Betts BC, St Angelo ET, Kennedy M, Young JW. Anti-IL6-receptor-alpha (tocilizumab) does not inhibit human monocyte-derived dendritic cell maturation or alloreactive T-cell responses. *Blood*. 2011;118(19):5340–5343.